An Efficient Maximum Power Point Tracking Controller for Photovoltaic Systems Using New Boost Converter Design and Improved Control Algorithm

TAMER T.N. KHATIB, A. MOHAMED and N. AMIN
Faculty of Engineering & Built Environment
University Kebangsaan Malaysia
Bangi 43600, Selangor
MALAYSIA
tamer_khat@hotmail.com, azah@eng.ukm.my, nowshad@eng.ukm.my

K. SOPIAN
Solar Research Institute, University Kebangsaan Malaysia
Bangi 43600, Selangor
MALAYSIA
ksopian@eng.ukm.my

Abstract: - This paper presents an efficient maximum power point tracking (MPPT) controller for a standalone photovoltaic (PV) generation system. To achieve an efficient MPPT controller, a new boost converter design and an improved MPPT algorithm are incorporated. In the proposed boost converter design, a passive regenerative snubber circuit is included to absorb the energy of stray inductance so as to reduce the IGBT switching losses. As for the improved MPPT algorithm, it is based on the curve fitting method which attempts to predict the power-voltage characteristic curve by a fourth order polynomial function. The predicted P-V curve strongly depends on the cell temperature and therefore the ambient temperature and solar radiation are used to track the maximum power point (MPP) of the PV module. Experimental results are given to verify the validity and performance of the MPPT algorithm which is embedded in a prototype MPPT controller. The experimental results showed that the proposed MPPT controller successfully tracked the MPP by giving an average tracking efficiency of 89.2%

Key-words: MPPT, photovoltaic systems, PV controller, boost converter, curve fitting

1. Introduction

The installation of photovoltaic (PV) generation systems is rapidly growing in response to concerns related to energy security and environmental issues such as global warming. PV generation system is considered as a clean and environmentally-friendly source of energy and it is operated either in standalone or grid connected modes. The standalone PV generation system is attractive as an indispensable electricity source for remote areas. However, PV generation systems have two major problems which are related to low conversion efficiency of about 9 to 12 % especially in low irradiation conditions and that the amount of electric power generated by PV arrays varies continuously with weather conditions. Therefore, considerable research is being carried out to increase the efficiency of PV systems by operating the system at maximum output power for any temperature and solar radiation level [1,2].

To maximize power produced by solar panels, a maximum power point tracking (MPPT) controller which is an electronic system is used to track the maximum power point of PV systems. A typical MPPT controller is shown in Fig. 1 in which it consists of a DC-DC boost converter and a microcontroller. The maximum power point (MPP) of a PV module can be detected by a microcontroller which is driven by an MPPT algorithm. Once the MPP is obtained, a triggering signal with a specific duty cycle is generated and used to trigger the boost converter switches in order to ensure that the converter operates as close as possible to the PV MPP.

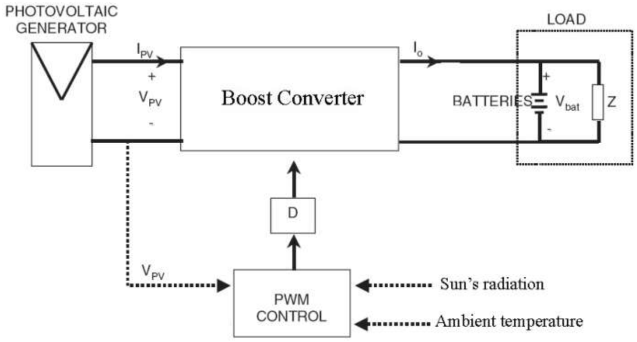

Fig. 1. Typical MPPT Controller

For an efficient MPPT controller, two considerations can be made, firstly by developing an improved algorithm for tracking the maximum power point (MPP) of PV systems and secondly by designing an efficient boost converter circuit which is an important component in the controller[3,4]. Boost converter may cause serious reverse-recovery problem and increase the rating of all devices. As a result, the conversion efficiency is degraded and may result in severe electromagnetic interference problem under this situation [5]. To overcome the severe reverse-recovery problem of high voltage diodes, voltage-clamped technique is manipulated in the converter design. However, this technique causes voltage stress on the switches and voltage gain is limited by the turn-on time of the auxiliary switch [6, 7]. Another problem in boost converter operation is the leakage energy of the storage inductor which is generated by the turning off action of the converter switches. It will result in a high-voltage ripple across the switch due to the resonant phenomenon induced by the leakage current. Therefore, to protect the converter switching devices, two mitigating actions can be taken, that is, by using a high voltage rating device with a snubber circuit and by depleting the inductor leakage energy. To increase the conversion efficiency of a boost converter, a new boost converter circuit has been designed by adding diodes and capacitors to the conventional converter circuit to transmit and sink the leakage energy of the inductor during transient switching.

For any PV module, there is a unique point on the current-voltage (I-V) and a power-voltage (P-V) curve, called as the MPP, in which at this point the PV system is said to operate at maximum efficiency and produces its maximum power output. The location of the MPP is not known but can be traced by using MPPT methods to maintain the PV array's operating point at its MPP. The MPPT methods can be classified as direct and indirect methods. The direct methods include those methods that use PV voltage and/or current measurements. These direct methods have the advantage of being independent from the priori knowledge of the PV generator characteristics. Thus, the operating point is independent of isolation, temperature or degradation levels. The direct methods include the techniques of differentiation, feedback voltage, perturbation and observation [8], incremental conductance, as well as fuzzy logic and neural network. The indirect methods are based on the use of a database of parameters that include data of typical P-V curves of PV systems for different irradiances and temperatures, or on the use of mathematical functions obtained from empirical data to estimate the MPP. In most cases, a prior evaluation of the PV generator based on the mathematical relationship obtained from empirical data is required. The methods belong to this category include the use of curve fitting [9, 10], look-up table, open-circuit and short circuit PV voltages [1,11]. In this paper, an improved indirect MPPT method is proposed by using the curve fitting technique. The present work introduces a hardware implementation of a microcontroller based MPPT controller for a PV system by incorporating an efficient DC-DC boost converter and an improved MPPT algorithm. The new boost converter circuit can produce smooth IGBT switching which consequently reduces the switching losses and increases the conversion efficiency. As for the proposed MPPT algorithm, it requires only parameters such as ambient temperature and solar radiation and therefore it makes measurement simpler for a cost effective controller.

2. Proposed Boost Converter Design

A boost converter is the front-end component of a PV system connected between a PV array and a load. It is basically a power converter with DC output voltage greater than its input voltage. It is a class of switching-mode power supply containing at least two semiconductor switches, a diode and a transistor and at least one energy storage element. Filters made of capacitors in combination with inductors are normally added to the output of the converter to reduce the output voltage ripple [12]. An inherent problem in boost converters is that it may cause serious reverse recovery problem which may increase the rating of devices and degrade the conversion. To increase the conversion efficiency, an improvement is made in the boost converter design. Fig.2. shows the proposed boost converter design. The converter consists of an inductor in the primary side (L), clamping diodes, D1,D2, capacitor C2 used to form a regenerative circuit to sink the reverse recovery current and an output filter circuit using diode, Do and capacitor, Co.

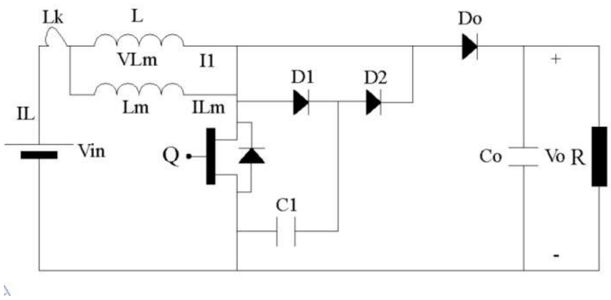

Fig. 2 Proposed boost converter

To describe the operation of the boost converter, four modes of operation are considered. Fig. 3 shows the triggering signal of the converter's switch operating at the four modes of operation.

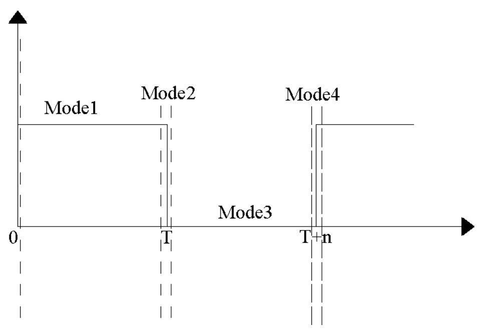

Fig. 3 Triggering signal

In the first mode of operation (mode 1), the switch Q is turned on and the inductor, L is charged by the voltage, Vin. Due to the magnetization in L, the current, ILm increases linearly. Since the input current, IL, is a square waveform, similarly the drain-source current, iDS will be of square wave shape. At the second mode of operation (mode 2), the switch Q is turned off and the current, IL will start to charge the parasitic capacitor of the switch Q. When the switch voltage is greater than the clamped capacitor voltage, VC1, the clamping diode, D1 will conduct and transmit the energy of the leakage inductor, LK into the clamped capacitor, C1. This capacitor is assumed to be large enough with favorable high frequency response so that its voltage, VC1 can be viewed as a stable DC output with low ripple for clamping the maximum value of the switch voltage. In addition, D1 should be a fast conductive device with voltage rating similar to the Switch Q.

As for the third mode of operation (mode 3), the switch is turned off and the reverse parasitic voltage of the output diode, Do decays to zero. At this time, Do starts to conduct and the rectifier diode, D2 is cut off. The series voltages, VLK and VLm will charge the output capacitor, Co and supply current to the load. Finally in the fourth mode (mode 4), the switch Q is turned on and the clamping diode, D1 is cut off promptly without reverse recovery current because it has a low voltage. The switch Q is turned on under zero current switching because the current, I1 is limited by the leakage inductor, Lk and it cannot derive any current from the inductor side or the passive regenerative snubber circuit side. This soft switching is helpful for reducing the switching losses.

2.1 Boost Converter Analysis

For boost converter analysis, the Mode 1 and Mode 3 operations for the ON and OFF switching states, respectively are taken into consideration. As the switching boost converter is time variant and topology variant, the defining equations of the circuit are put in the following forms [12].

At Mode 1, during the time interval of $0 < t < T$, it can be observed that,

$$L\frac{dI_L(t)}{dt} = V_{in}(t) \tag{1}$$

$$C_o\frac{dV_{C_o}(t)}{dt} = -\frac{V_{C_o}(t)}{R} \tag{2}$$

At Mode 3, during the time interval of $T < t < T+n$, the equations for the circuit are defined as,

$$L\frac{dI_L(t)}{dt} = V_{in}(t) - V_{C_o}(t) \tag{3}$$

$$C_o\frac{dV_C(t)}{dt} = I_L(t) - \frac{V_{C_o}(t)}{R} \tag{4}$$

Define a time variant control input variable, $\delta(t)$ which is given by,

$$\delta(t) = \begin{cases} 1, & 0 < t < T \\ 0, & T < t < T+n \end{cases}$$

By considering $\delta(t)$ and substituting it into equations (3) and (4), the defining equations of the time variant and topology variant circuit becomes,

$$L\frac{dI_L(t)}{dt} = V_{in}(t) - [V_C(t)x(1-\delta(\acute{t}))] \quad (5)$$

$$C_o\frac{dV_{C_o}(t)}{dt} = [I_L(t)x(1-\delta(\acute{t}))] - \frac{V_{C_o}(t)}{R} \quad (6)$$

To perform DC steady state and AC small signal analyses, the variables $V_c, I_L, V_{in}\ and\ \delta$ are defined as having two components which are the DC component and the corresponding perturbation component [12]. If the DC components are represented by the letters with non hat symbol and the perturbation components are represented by the letters with hat symbol, (5) and (6) become,

$$L\frac{d\,\hat{i_L}(t)}{dt} = V_{in} + \widehat{V_{in}}(t) - (V_{C_o} + \widehat{V_{C_o}}(t))\left((1-D) - \left(1-\hat{d}(t)\right)\right) \quad (7)$$

$$C\frac{d\,\widehat{V_o}(t)}{dt} = I_L + \widehat{I_{iL}}(t)\left((1-D) - \left(1-\hat{d}(t)\right)\right) - \frac{V_C + \widehat{V_C}(t)}{R} \quad (8)$$

where, D is the duty cycle.

To perform DC steady state analysis, let $\widehat{V_{C_0}}, \widehat{I_L}, \widehat{V_{in}}\ and\ \hat{d} = 0$ and $V_{c_o} = V_o$. Then (7) and (8) become,

$$V_{in} - Vo(1-D) = 0 \quad (9)$$

$$I_L(1-D) - \frac{V_o}{R} = 0 \quad (10)$$

From (9), the relation between the input and the output voltages of the boost converter will be:

$$\frac{Vo}{V_{in}} = \frac{1}{1-D} \quad (11)$$

From (10) we get

$$I_L = \frac{V_{in}}{R_{load}[1-D]^2} \quad (12)$$

Assuming that the converter is ideal in which output power is equal to the input power, $P_{out} = P_{in}$, we get

$$V_{in}\,I_{in} = V_o\,I_o \quad (13)$$

Substituting (11) into (13), we get the voltage and current gain equation of the boost converter which is given by,

$$\frac{V_{in}}{V_o} = \frac{I_o}{I_{in}} = [1-D] \quad (14)$$

3. Proposed MPPT Method for PV System

The MPP is the extreme value of the P-V curve at specific solar radiation and ambient temperature values. To predict the P-V curve of a PV generator, the nonlinear characteristic of the PV generator can be modeled off-line based on mathematical equations or numerical approximations [13]. To achieve an accurate fitting of the P-V curve, a polynomial function of the fourth degree is used and it is given by,

$$P_{pv} = P_1 V_{pv}^{\ 4} + P_2 V_{pv}^{\ 3} + P_3 V_{pv}^{\ 2} + P_4 V_{pv} + P_5 \quad (15)$$

Fig. 4 shows a comparison of the P-V curve obtained from using the fourth order polynomial function and the actual P-V curve

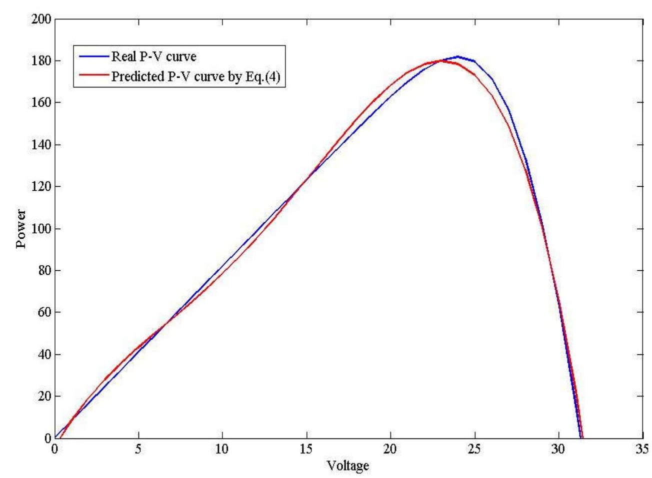

Fig. 4. P-V prediction by the fourth order polynomial function

The results show that the P-V curve predicted from using the fourth order polynomial function is more accurate as compared to using the third order polynomial function as proposed in [9,10]. Thus, the fourth order polynomial function is used to predict the P-V curve.

After obtaining an accurate prediction of the P-V curve using the fourth order polynomial P-V function, this function ($P_{pv} = f(V_{pv})$ is then used to determine the coefficients of the fitting function. In this case, the inputs of this function (equation 15) are the PV module's power and voltage and the outputs are the five coefficients ($P_1, P_2 \dots P_5$).

Considering the fact that the PV module's voltage depends on the cell temperature in which it varies with the sun's radiation, it is considered that the PV power is also a function of the temperature. The cell temperature can be calculated from the nominal operation condition temperature (NOCT) which is the temperature of the cell at 800W/m^2 and 20 ^{o}C ambient temperature [1]. The cell temperature is given by,

$$T_{cell} - T_{ambient} = \frac{NOCT-20}{800} G \quad (16)$$

Using the MATLAB based PV model which is represented by a current source function in terms of PV voltage, irradiance and cell temperature [15], a large sampling of P-V curves under wide range of temperatures (0 ^{0}C – 100 ^{0}C) are obtained. The P-V curves at various temperatures are plotted as shown in Fig.5 and fitted with the fourth order P-V polynomial function by using the MATLAB fitting function (P=polyfit(x,y,N)).

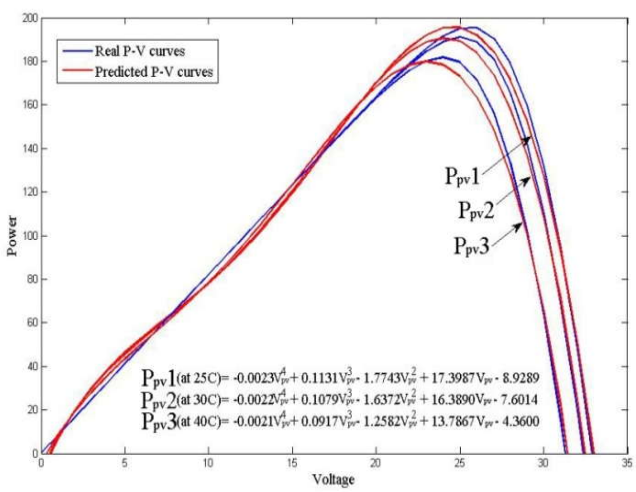

Fig. 5 P-V predicted functions at different temperatures

From the derived P-V curves, the coefficients with respect to the various cell temperatures are obtained. Table 1 shows some samples of the PV coefficients at temperatures 20 ^{0}C – 40 ^{0}C. From these coefficient values, each coefficient can be plotted with respect to the cell temperature. Figs. 10a, 10b, 10c, 10d and 10e show the plots of the coefficients P_1, P_2, P_3, P_4 and P_5 verses the cell temperature, respectively.

TABLE I
PV COEFFICIENTS AT DIFFERENT TEMPERATURES

T_{cell}	P1	P2	P3	P4	P5
0	-0.0021	0.1088	-1.91	19.35	-12.37
10	-0.0023	0.1165	-1.9638	19.1791	-11.6146
20	-.0023	.1161	-1.8715	18.1767	-10.0084
30	-.0022	.1079	-1.6372	16.3890	-7.6014
40	-.0021	.0917	-1.2582	13.7867	-4.360
50	-0.0018	0.0673	-0.7303	10.3455	-0.2450
65	-0.0014	0.0350	-0.0596	6.0996	4.6844
70	-8.67e-4	-0.0053	0.7560	1.0387	10.4486
80	-2.34e-4	-0.0536	1.7164	-4.8372	17.0476
90	5.15e-4	-0.1099	2.8217	-11.528	24.4814
100	0.0014	-.1742	4.0720	-19.034	32.75

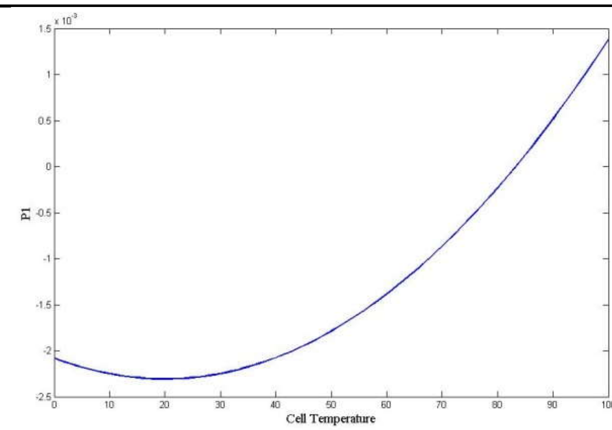

Fig. 10a: Coefficient P_1 vs cell temperature

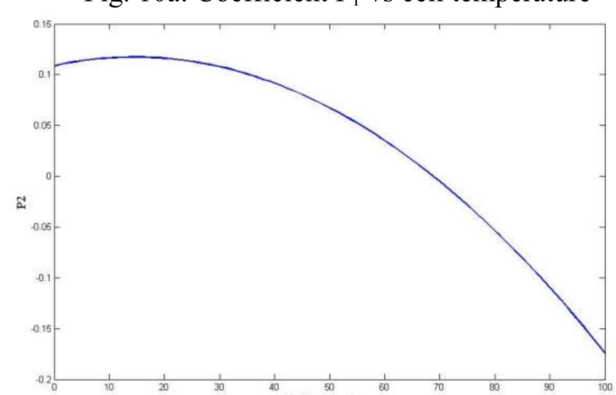

Fig. 10b: Coefficient P_2 vs cell temperature

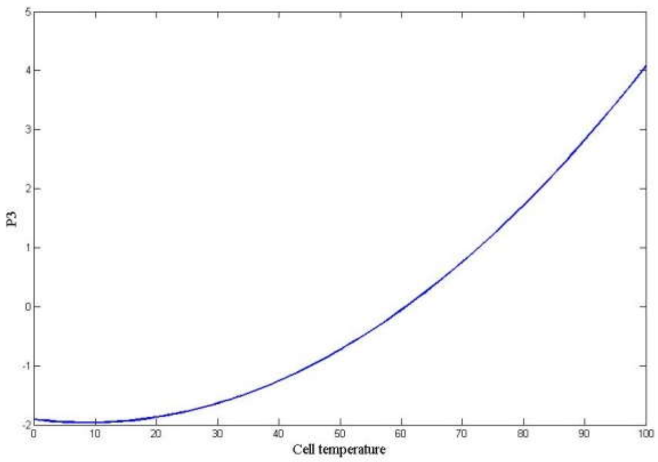

Fig. 10c: Coefficient P_3 vs cell temperature

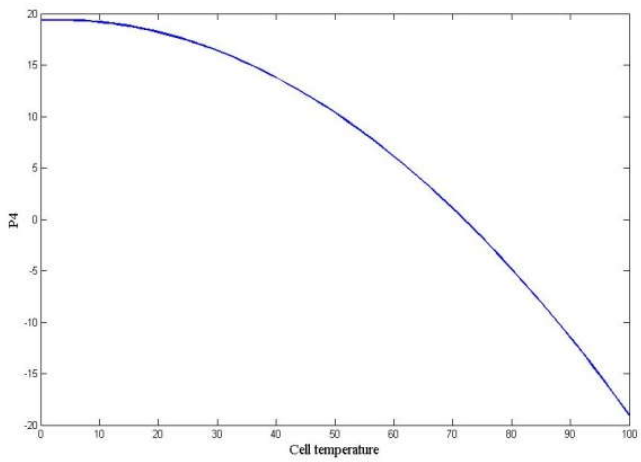

Fig. 10d: Coefficient P_4 vs cell temperature

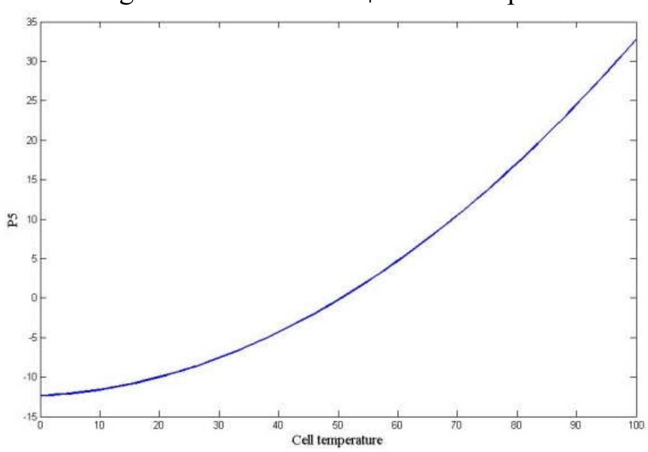

Fig. 10e: Coefficient P_5 verses cell temperature

From Figs. 10a-10e, each coefficient can be described individually as a function of the cell temperature ($P_N = f(T_{cell})$). By using the MATLAB function (P=polyfit(x,y,N)) again, the coefficient function for each curve can be derived. It is noted that the derived coefficient functions are polynomial of the second degree and are given as follows:

$$P_1 = 5.75 * 10^{-7} T_c{}^2 - 2.3 * 10^{-5} T_c - 2.1 * 10^{-3} \quad (17)$$

$$P_2 = -4 * 10^{-5} T_c{}^2 + 1.17 * 10^{-3} T_c + .101 \quad (18)$$

$$P_3 = 7.25 * 10^{-4} T_c{}^2 - 1.26 * 10^{-2} T_c - 1.9 \quad (19)$$

$$P_4 = -4.1 * 10^{-3} T_c{}^2 + 2.37 * 10^{-2} T_c + 19.35 \quad (20)$$

$$P_5 = 4.18 * 10^{-3} T_c{}^2 + 3.4 * 10^{-2} T_c - 12.4 \quad (21)$$

where Tc is the cell temperature.

Fig. 11 shows the proposed MPPT algorithm in terms of a flowchart. In the method, an approximate fourth order polynomial function of the P-V curve is first obtained and then used to derive the coefficient functions of the P-V curve in terms of the cell temperature. The tracking process starts with sensing the ambient temperature and the sun's radiation. The reference temperature, irradiation and rated load voltage, $G_{refrence}, T_{cell_{refrence}}$ and $NOCT$ are obtained from the PV module's data sheet. Then, the cell temperature is calculated by using (16). Using the cell temperature value, the coefficients are calculated using (17) – (21).

To determine an optimum PV voltage at which the PV power is equal to its maximum value from the fourth order polynomial function, the condition $\frac{dP_{pv}}{dV_{pv}} = 0$ is considered. Consequently, we get,

$$\frac{dP_{pv}}{dV_{pv}} = 4P_1 V_{pv}{}^3 + 3P_2 V_{pv}{}^2 + 2P_3 V_{pv} + P_4 = 0 \quad (23)$$

The PV module's voltage that is sensed by the controller is used by substituting it into (23) so as to determine the dP_{PV}/dV_{PV} value. If it is equal to zero, it means that the PV generator is operated at its optimum voltage whereas if it is greater than zero, the process of searching the optimum voltage is repeated by incrementing or decrementing the PV voltage with a constant, C set at a value of 0.1. After finding the optimum PV voltage, the optimum duty cycle is calculated.

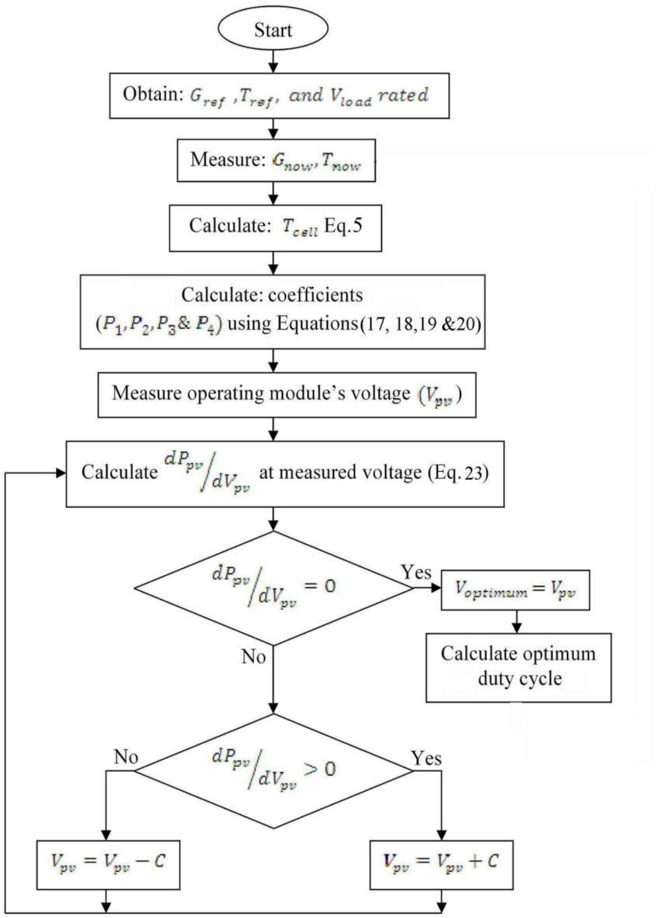

Fig. 11: MPPT Algorithm

4. Experimental Results

A prototype of the microcontroller based MMPT has been designed and developed as shown in Fig. 12. The controller circuits diagram is shown in Fig.13. The MPPT controller consists of boost converter with snubber circuit, microcontroller circuit and feedback sensors. The proposed MPPT algorithm has been programmed on the PIC16F778 microcontroller. This microcontroller has 7 data reading ports and a pulse width modulation (PWM) port. During the tracking, the microcontroller reads three input readings; PV module's voltage, ambient temperature and solar radiation. Based on these readings the optimum duty cycle of the triggering signal is calculated. The MPPT controller was tested by connecting it to a standalone PV system installed at the university campus site as shown in Fig.14. The PV system consists of a 350 Watt PV module and a chargeable battery 180 Ah, 24 V. A 24V/240V inverter is connected between the battery and loads comprising of an osmosis pump, lights and power plugs for common uses. Table 2 shows the specification of the boost converter's devices.

Fig. 12: Prototype of the MPPT controller

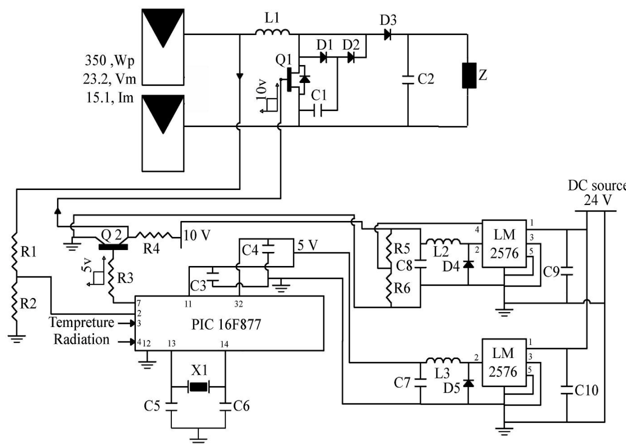

Fig. 13 Circuit diagram of the MPPT controller

Fig. 14: Testing site

TABLE II
BOOST CONVERTER SPECIFICATION

Label	Description/ Value
Q1 (IGBT)	MOSFET , TO-247AC. 75 V
L1	2 mH, 30 A
C1	6.8 µF, 100V
C2	680 µF , 100 V
D1, D2 and D3	SCHOTTKY diodes , TO-220, 20 A, 80 V

The MPPT controller is connected between the PV modules and the battery. Thus, the PV modules charge the battery through the MPPT. A charge controller is also connected to protect the battery from being over charged or over discharged. During the MPPT controller testing, the solar radiation, ambient temperature, batteries' state of charge and MPPT output voltage and current were measured. Fig. 15 shows the solar radiation curve during the testing day which was a sunny and clear day. The peak sun shine hours is 5.7 hours and consequently the extracted energy form the PV modules is 1995 KWh. Fig. 16 shows the ambient temperature profile on the testing day in which the temperature was 23.5 °C in the morning and then reached a peak value of 32.5 °C
in the mid afternoon.

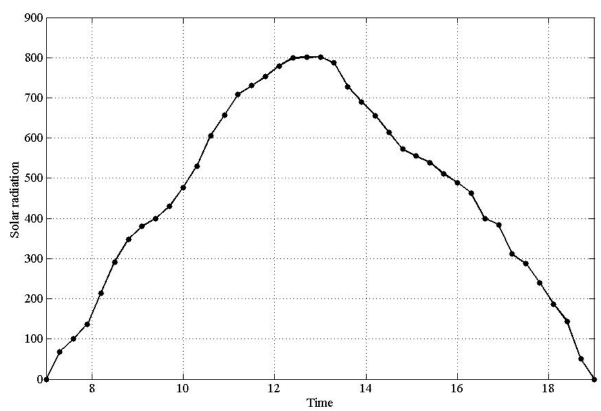

Fig.15: Solar radiation curve during the testing day

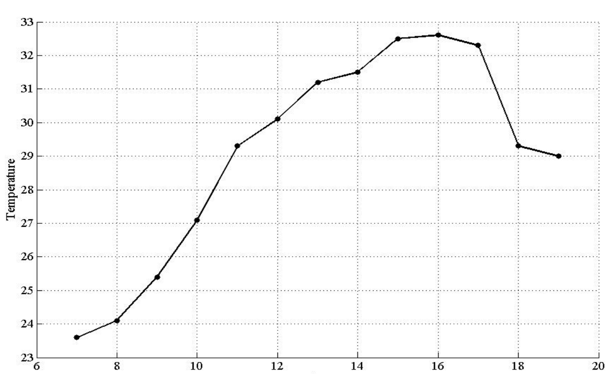

Fig. 16: Ambient temperatures during the testing day

The MPPT output voltage and current were also measured so as to determine the MPPT output power. Fig. 17 shows the voltage and current profiles during the testing day.

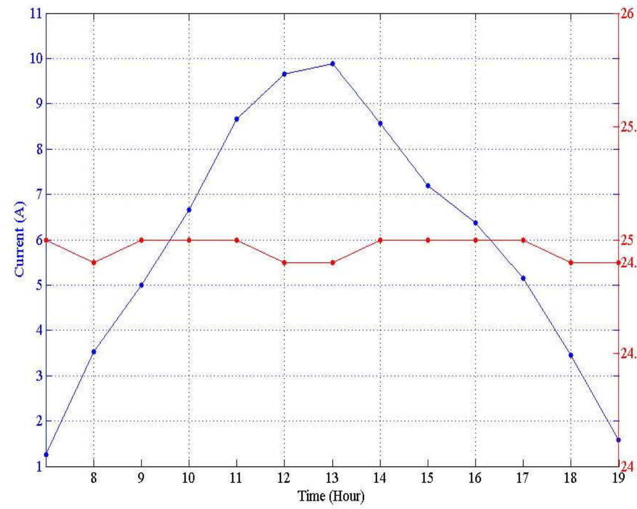

Fig. 17: MPPT output voltage and current during the testing day

From the MPPT output voltage and current, its output power and efficiency are calculated. The efficiency of a MPPT can be defined as the extracted power from the PV module multiply by the boost converter conversion efficiency and divided by the theoretical maximum power at the same weather conditions [16]. Based on this definition, the MPPT's efficiency during the testing day was calculated and plotted as shown in Fig. 18. It is noted that the efficiency varies between 88% - 90% with an average efficiency of 89.2%. Due to varying ambient temperatures and solar radiation, the MPPT efficiency is affected. Fig. 19 and 20 show the effect of ambient temperature and solar radiation on the MPPT efficiency, respectively. From Fig. 19, it is clear that the MPPT's efficiency decreases when the ambient temperature increases. Thus, it can be concluded that MPPT has better efficiency when operating at moderate temperatures. It is noted that low sun radiation affects the tracking efficiency negatively (Fig. 20). Thus, tracking efficiency may be degraded when the solar radiation becomes lower than 300 W/m^2.

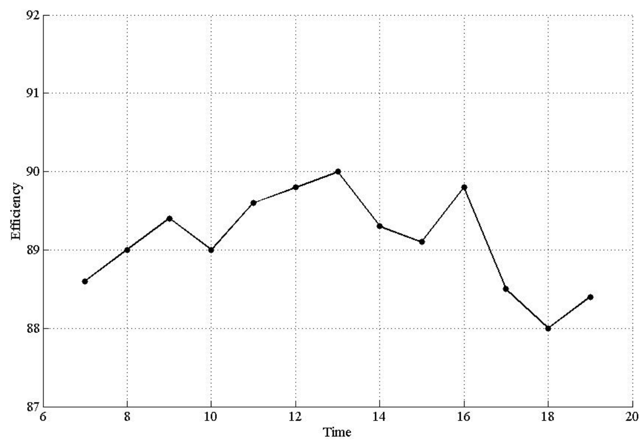

Fig. 18: Tracking efficiency

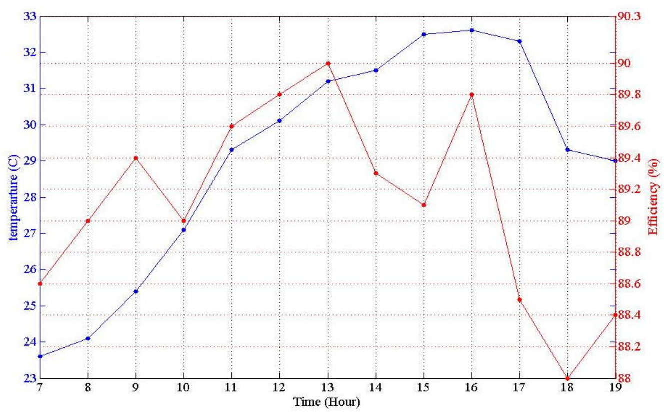

Fig. 19: Effect of temperature on MPPT's efficiency

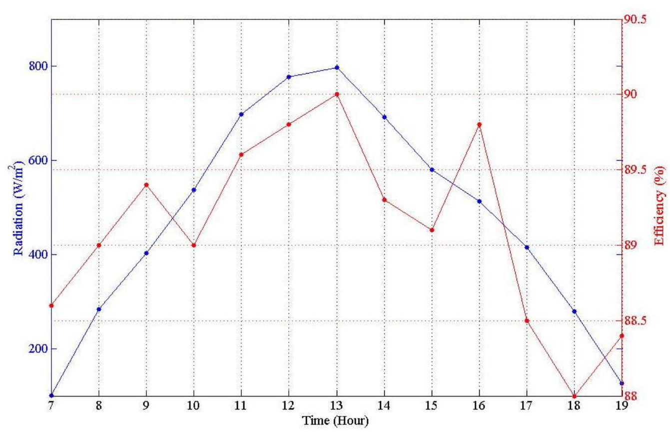

Fig. 20: Effect of solar radiation on MPPT

Fig. 21 shows the batteries' state of charge (SOC) during the testing day in which the initial SOC is 56% and the final SOC is 89.6%.

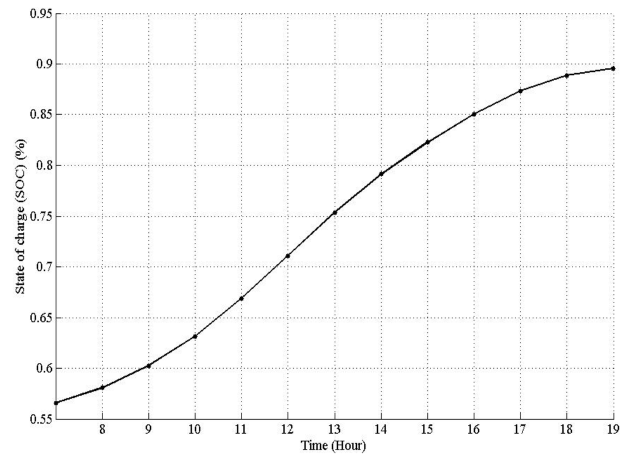

Fig. 21: Batteries' state of charge during testing

Figs.22 and 23 show the PV system's performance with and without MPPT. To do this comparison the system was operated for short while with and without MPPT. The values of solar radiation in both cases are shown at the top of the columns. Since the solar radiation values are very close to each other, a comparison for the performance of the system with MPPT and without MPPT can b obtained. See Fig (22). The MPPT increases the extracted power from the PV modules and consequently increases the system efficiency (Fig.22). Fig.23 shows a comparison of the PV module's output voltage for the case of with and without MPPT. It is noted that the voltage profile is more stable with MPPT than the voltage profile without MPPT.

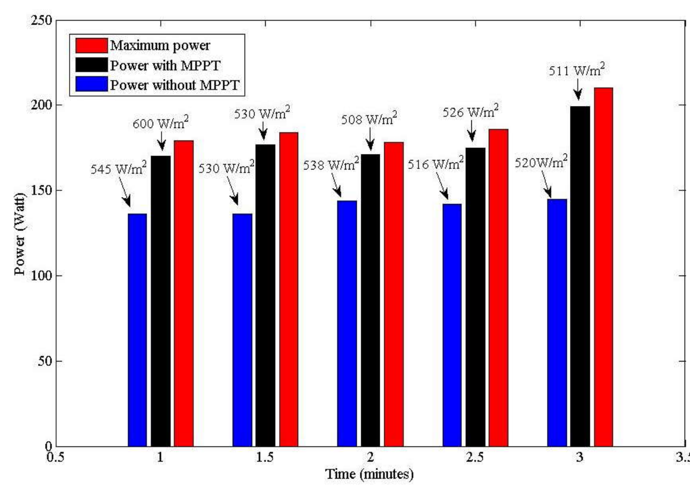

Figure 22 PV system output power with and without MPPT

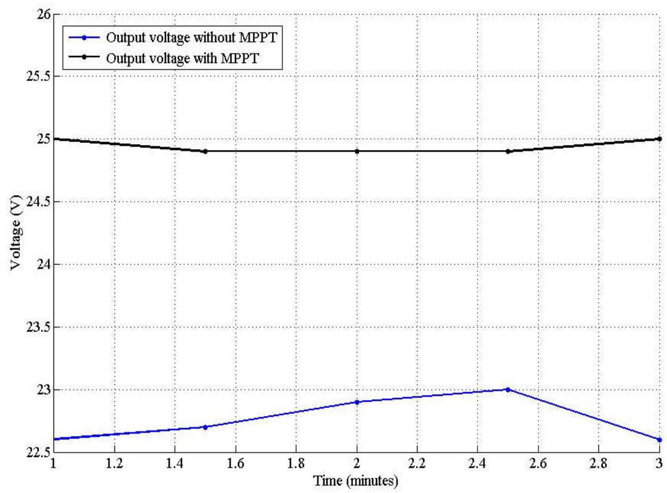

Figure 23 Output voltage profile with and without MPPT

Simulations were also carried out to compare the performance of the conventional boost converter and the proposed boost converter. The simulation results in terms of the boost converter conversion efficiency are shown in Fig. 24. From the figure, it can be seen that the conventional boost converter reach its MPP in 0.4 sec and the conversion efficiency is 88.2%. On the other hand, the proposed boost converter reaches it's MPP in 0.6 sec with conversion efficiency higher than the conventional one (92.6 %). Thus, by adding a snubber circuit in the boost converter, better soft switching of the converter's switches can be achieved and the conversion efficiency increases by 4.4 %.

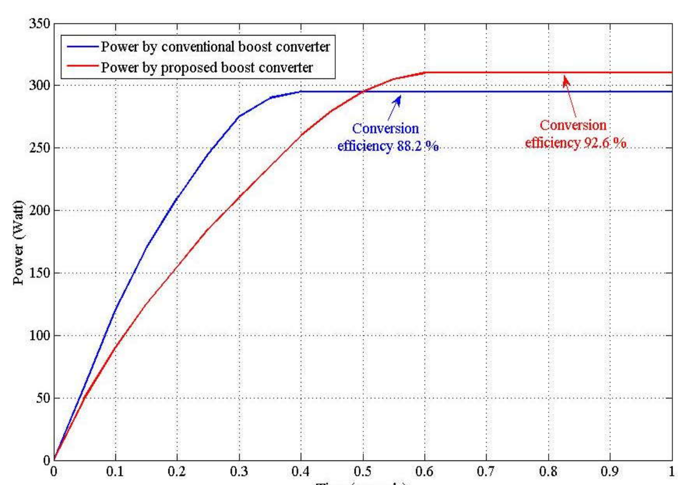

Figure 24 Comparison between the conventional boost converter and the proposed boost converter

5. Conclusion

An efficient MPPT controller has been developed by incorporating a new DC-DC boost converter design and an improved MPPT algorithm based on the indirect curve fitting technique. The MPPT algorithm approximates the P-V curve by representing it with a fourth degree polynomial function in terms of ambient temperature and sun's irradiation. The developed MPPT algorithm is programmed in a microcontroller based MPPT controller and tested on an existing PV system. Experimental test results showed that the proposed MPPT gives an average tracking efficiency of 89.2%. It is also shown that the tracking efficiency is lowered by 6% during high temperature and low radiation conditions. An advantage of the proposed MPPT controller is that it is cost effective and simple because it does not require current measurements during MPP tracking.

References

[1] Salas, V., A.Barrado, E. O., lazaro, A. (2006). *Review of the maximum power point tracking algorithms for stand-alone photovoltaic systems*. Solar Energy Materials & Solar Cells, Vol.90, pp:1555–1578.

[2] I. Güney, N. Onat, Technological Status and Market Trends of Photovoltaic Cell Industry, *WSEAS Transactions on Electronics*, Vol.5, Iss.7, pp.303-312, 2008.

[3]Jui-Liang Yang , Ding-Tsair Su , Ying-Shing Shiao, Research on MPPT and single-stage grid-connected for photovoltaic system, WSEAS TRANSACTIONS on SYSTEMS, v.7 n.10, p.1117-1131, October 2008

[4]Liu Liqun , Wang Zhixin, A variable voltage MPPT control method for photovoltaic generation system, WSEAS Transactions on Circuits and Systems, v.8 n.4, p.335-349, April 2009

[5] Mohan, N., Undeland, T. M., Robbins. W. P.,(1995), Power Electronics: Converters, Applications, and Design. Wiley

[6] Jovanovic. M. M. , Jang, Y.,(1999), A new soft-switched boost converter with isolated active snubber, IEEE Trans. Ind. Appl. Vol. 35, pp. 496–502.

[7] Duarte, C. M. C. , Barbi, I.,(2002), An improved family of ZVS-PWM active clamping DC-to-DC converters, IEEE Trans. Power Electron.,Vol. 17, no. 1, pp. 1–7.

[8] Tafticht, T., Doumbia, M., Che´riti, A. (2008). *An Improved Maximum Power Point Tracking Method*

for Photovoltaic Systems. Renewable Energy. Vol.33, pp: 1508–1516

[9] Takehara, N., Kurokami, S.,(1997) *Power control apparatus and method and power generating system using them*. Patent US5,654,883.

[10] Phang, J.C.H., Chan, D.S.H. , Phillips, J.R. ,(1984). *Accurate analytical method for the extraction of solar cell*, Electron. Lett. Vol.20, pp:406–408.

[11] Faranda, R. , Leva, S. (2008). *Energy comparison of MPPT techniques for PV Systems*. WSEAS Transactions on Power Systems, Vol. 3, pp:446-455

[12] Xu, J.,(1991), An Analytical Technique for the Analysis of Switching DC-DC Converters, International Symposium on Circuits and Systems ,Vol.2, pp. 1212 - 1215.

[13] Hamdy, M.A. , (1994). *A new model for the current-voltage output characteristics of photovoltaic modules*, J. Power Sources, Vol. 50 , pp:11–20.

[14] Takashima, T. , Tanaka, T., Amano, M. , Ando, Y., (2001). *Maximum output control of photovoltaic (PV) array*, Intersociety Energy Conversion Engineering Conference and Exhibit (IECEC), 35th, pp. 380–383.

[15] Walker, G.,(2001). *Evaluating MPPT converter topologies using a MATLAB PV model," Journal of Electrical & Electronics Engineering*, Australia, IEAust, vol.21, pp.49-56.

[16] Enrique, J.M. , Andujar, M.A. Bohorquez. (2010). *A reliable, fast and low cost maximum power point tracker for photovoltaic applications*. Solar Energy Vol.84, pp:79-89.